Title:

Nonlinear optical effects and optomechanical oscillations in hollow Whispering Gallery Mode microresonators: coexistence, suppression, amplification and route to chaos

Authors:

Gabriele Frigenti[b], Daniele Farnesi[b,*], Xavier Roselló-Mechó[a], Andrea Barucci[b], Fulvio Ratto[b], Martina Delgado-Pinar[a], Miguel V. Andrés[a], Gualtiero Nunzi Conti[b] & Silvia Soria[b]

* Corresponding author: Institute of applied physics "Nello Carrara" (IFAC) – CNR, Via Madonna del Piano, 10, 50019 Sesto Fiorentino (FI), Italy.
E-mail addresses: d.farnesi@ifac.cnr.it (D. Farnesi).

Affiliations:

a - Department of Applied Physics and Electromagnetism-ICMUV, University of Valencia, Burjassot, Spain.
b - CNR-IFAC Institute of Applied Physics "N. Carrara", 50019, Sesto Fiorentino, Italy.

Abstract:

Whispering Gallery Mode (WGM) hollow microcavities turn out to be the site of an extremely rich and complex phenomenological scenario when pumped with a continuous-wave laser source. The coexistence of numerous non-linear and optomechanical effects have been reviewed in this paper. In our previous works we have investigated and described non-linear emissions as the stimulated Brillouin and Raman scattering, the degenerated and non-degenerated Kerr effects, such as four wave mixing. These effects happened concomitantly to parametric optomechanical oscillations which are the consequence of the radiation pressure. We have confirmed the regenerative oscillation of acoustic eigenmodes of the cavity leading to parametric instabilities and the activation of optomechanical chaotic oscillations. Finally, we have demonstrated that the blue-side excitation of WGM resonances lead to the chaos transition with a spectral evolution depending on the cavity size.

Keywords: SiO_2, Optical properties, Nonlinear Phenomena

Main Text:

Whispering gallery mode resonators (WGMR), through the combination of their circular symmetry and total internal refraction, have shown to be an excellent platform for confining the light in very small volumes with ultra high Q-factors [1,2]. The related high photon density and long lifetime allow to study, from the fundamental point of view, the light matter interactions such as Kerr and stimulated phenomena like Raman scattering (SRS) [3,4]. Different WGMR geometries, both solid and hollow, as spherical, toroidal, and bottle-shaped, with a large variety of host materials, have attracted a great interest in the last decades [5]. The rich spectrum of sharp optical resonances, regardless of the specific WGMR geometry, is the key feature for their implementation in various applications. The newest members of this family of cavities are the microbubble resonators (MBR) [6] which are fabricated heating a pressurized silica capillary [7,8], mimicking on the micro-scale the procedure followed by a glassblower. The obtained hollow structure allows flowing liquids or gas inside the WGMR, thus making them suitable for sensing applications (as refractometers [7,9], mass sensors [10], temperature [11], pressure [12] and viscosity [13]) and, in addition, gives the possibility of tailoring both dispersion [14] and resonant properties [15,16]. Only lately, the MBR have been also used for fundamental studies in nonlinear optics [17] and lasing [18]. Last but not least, MBR have demonstrated the ability to sustain not only photons, running in their optical modes, but also optical and acoustic phonons of the material making up the resonator [19], and low frequency mechanical modes featuring an MBR overall vibration with the expansion or bending of walls [20]. The coherent interaction of light photons and acoustic phonons results into an inelastic scattering process, the Stimulated Brillouin Scattering (SBS) [21,22], which is enhanced due to the overlap of both waves inside this dual photonic-phononic or "phoxonic" cavity [23,24]. It is a pure gain process, automatically phase-matched, with a large gain coefficient but a small gain bandwidth [25]. Due to its narrow bandwidth, the SBS frequency shift must be equal to the free spectral range (FSR) of the WGMR, imposing strict conditions on WGMR geometries [26–28]. In MBRs, this condition can be bypassed thanks to their eccentricity, which removes the modes degeneracy, and by using high order modes [29,30] with vertical

FSR smaller than the fundamental one [31–33]. In bulk silica, the acoustic phonons responsible for SBS are in the GHz range [19,34]. On the other hand, the mechanical modes in the silica MBR, have lower frequencies, in the range of hundreds of kHz to tens of MHz [4]. These oscillations, which are the mechanical eigenfrequencies of the cavity [35–37], present a threshold behavior and result to be regenerative without the need of a pump wave external modulation. The mechanical modes are excited through the radiation pressure (RP) produced by the photons running in the optical modes [36,38]. At first, such effects have been observed in WGM toroids [39,40], then in spheroids [35], solid microbottles [37] and finally in MBRs. In all these WGMR geometries, the interplay between an optical mode (frequency ω_R), excited by a slightly detuned laser source (frequency ω_L), and a mechanical mode (frequency Ω_m), activated by the radiation pressure, produces a sinusoidal perturbation of the resonator optical length with the same frequency Ω_m. This oscillation generates two sidebands waves at frequencies $\omega_L - \Omega_m$ (Stokes) and $\omega_L + \Omega_m$ (antiStokes band). If one of the sidebands is perfectly resonant with the WGM (i.e. if $\omega_L - \Omega_m = \omega_R$ or $\omega_L + \Omega_m = \omega_R$), the sideband wave is guided and enhanced by the WGM. The laser source detuning determines if the interaction has a positive or negative feedback, respectively amplifying or quenching the mechanical mode. A depletion of the sideband wave and the energy removal from the mechanical mode (negative feedback) is achieved if the laser source is red-detuned ($\omega_L < \omega_R$) and the anti-Stokes band is resonant. The worst configuration, which can be exploited to efficiently suppress the thermal oscillations, occurs by moving the energy on the laser wave. Instead, an enhancement of the sideband amplitude and an increase of the mechanical mode energy (positive feedback) is achieved if the laser source is blue-detuned ($\omega_L > \omega_R$) and the Stokes band is resonant. The best configuration to get optomechanical oscillations (OMOs) [41] occurs by moving the energy on the Stokes sideband wave. The OMOs are read through the shift induced into the optical resonance. In particular, an oscillation is induced in the resonance, around its initial position, causing a modulation of the WGMR at the frequency of the mechanical mode (Ω_M). Due to the low activation threshold, OMOs were also studied in combination with nonlinear optical effects (NLOE) which typically start when the cavity is already oscillating. These two processes compete with each other on activation [20,42] and their coexistence is not in general guaranteed, in fact, configurations where one is enhanced at the expense of the other are possible. Furthermore, both in toroids and spheroids [35,40], it was shown that launching high input powers produces an erratic behavior, which is experimentally observed through the formation of a period spectral doubling. Finally, an optomechanical study demonstrated the presence of chaos mediated stochastic resonances and chaos transfer in a WGM microtoroid [43].

This review reports on the temporal behavior of the nonlinearities in WGM bubble resonators focusing our attention on the evolution of the standard optomechanical regime towards the chaotic behavior, in presence of other NLOE. First, we have demonstrated that the thin walls MBR are very efficient for SBS emission and show a rich nonlinear scenario. In particular, compared to refs [16,19], we have used MBR with thinner walls (2–4 instead of 10–15 μm) to observe simultaneous SBS and FWM (as opposed to ref.[16]) and SBS lines acting as a pump in SBS-uncoupled FWM processes. The SBS efficiency has resulted more than one order of magnitude higher compared to the previous studies. The MBR, as thin spherical shells, not only satisfy different phase matching and multi-resonant conditions required by the above mentioned NLO effects, but also excite parametrical optomechanical oscillations.

To study these effects is necessary to thermally self-lock the resonant mode to the pump laser, by tuning the laser from high to low frequencies [44]. For certain locking conditions (high pump power) the mechanical oscillation was amplified and the nonlinear phenomena were suppressed [42]. In this case, we observed single mode mechanical oscillations and OMO oscillations which continue as long as the pump power is maintained, in agreement with Braginsky theory [38]. MBRs are not only able to support a very dense mechanical mode spectra, but also allows to observe their evolution towards chaotic behaviors. It is worth to notice how our studies have been performed using a continuous wave (CW) source without external feedback, modulation, delay or periodic perturbation.

We have shown two different routes to chaos and the chaos transfer, within the same MBR, between a high-power pump WGM, which excite the OMO, and a low-power probe WGM which will follow the same route as the pump. This analogy with microtoroids shows that the chaotic motion induced by the RP is an intrinsic property of the optical cavity [40].

In Fig.1, we show the experimental setup used to study both nonlinear optical effects and opto-mechanical oscillations of MBRs. The output of a tunable laser source at 1550 nm (TL,Nettest TUNICS-Plus) is increased with an erbium-doped fiber amplifier (EDFA, IPG Photonics) and, after passing an attenuator (ATT), a polarization controller (PC) and a circulator (CIRC), for extracting the backward-direction signal), is launched into home-made tapered fiber (with a minimum waist cross-section diameter of 2 μm) to excite the WGMs of an MBR. The transmission of the resonator-coupler system is then split and sent to an optical spectrum analyzer (OSA, Ando AQ6317B, resolution: 20 pm) and a fast photodetector (PD, Thorlabs PDA400), connected either to an oscilloscope (OSC, Tektronix DPO7104), or to an electrical spectrum analyzer (ESA, Rohde & Schwarz FSL, 9 kHz-6 GHz). The optical power sent to the MBR is split before the taper fiber and monitored with a power meter (PM, Ando AQ2140).

In our experiment, we used MBRs with a diameter ranging from 420 to 780 μm and wall thicknesses ranging from 2 to 6 μm. They were fabricated using an electrical arc discharge technique [7] and the wall thicknesses were estimated through a well-known model based on the mass conservation during the fabrication process [45]. The MBR characterizations were performed at low input power of the wavelength-scanning laser source in order to avoid nonlinear phenomena and the

thermal broadening of the resonances. The Q-factor values ranging between 10^6 and 10^7, the free spectral range (FSR) roughly from 100 to 200 GHz (with diameter between 700 and 400 μm, respectively).
The MBR diameters have been chosen based on their dispersion. In these cavities, at 1550 nm, the geometrical dispersion is normal and large, whereas the material dispersion is anomalous and larger than other one. The total dispersion is anomalous, also for very large MBR, with values in the order of several hundreds of kHz [33]. In our experiments, we started by identifying resonances showing passive thermal locking [44] and then increased the input power. Thermal locking allowed the laser to stay blue-detuned with the resonance and increase the resonator energy build-up, permitting to exceed the activation threshold of non-linear and OMO phenomena. In [17], by launching a pump power of 80 mW into a 475 μm diameter MBR, we have obtained in backward direction a SBS Stokes line shifted of 11,2 GHz (Fig.2a). Increasing the launched power up to 200 mW, in a MBR of diameter about 675 μm and wall thickness of about 2 μm, a cascaded SBS up to the 4th order with Stokes lines shifted by 11, 22, 33 and 44 GHz has been observed (Fig.2b). By tuning the pump wavelength, we have achieved the best efficiency (up to 17%) in the 2nd order SBS lasing.

In forward direction, we have also detected SRS contemporaneously to SBS, whose Stokes line are separated by 13 THz (110 nm) from the pump (as shown in fig.2c) and FWM, from the second order Brillouin laser line, separated by a FSR (Fig.3a). Instead, in backward direction, we achieved two sets of Stokes and anti-Stokes lines, the first separated by one FSR and the second by a non-integer multiple of the FSR from the 2nd order stimulated Brillouin laser line (Fig.3b).

As previously mentioned, in addition to the dense optical spectrum, MBRs have a complex mechanical modes spectrum. In order to calculate their mechanical eigenmodes, we have performed numerical simulations [20] using FEM in COMSOL Multiphysics. Ideally, these modes belong to three different families: 1) Radial breathing modes (m = 0) correspond to non-degenerate extension-compression of the spherical shell with a cylindrical symmetry respect to the longitudinal axis; 2) Rocking modes (m = 1) correspond to a lateral bending of the cavity displaying double degeneracy with a mutual orientation of 90°; 3) Wineglass modes (m > 1) exhibit more nodes and occasionally a sharp localization along the MBR equatorial circumference and maintaining double degeneracy at angles depending by the mode order. We have reported the effect of the microbubble diameter on a representative selection of mechanical modes (Fig. 4a) and identified two different frequency ranges, one for sub-millimetric MBR (70–700 kHz) and the other for MBR with diameters smaller than 600 μm (1–60 MHz). Figure 4 (b) and (c) show the mechanical oscillations respectively for the taper coupled at the equator of a MBR (475 μm in diameter) and laterally shifted along the MBR axis, achieved with a launched pump power of 72 mW. When only one mechanical mode is excited (Fig. 4b), the first sharp peak corresponds to a mode at 3.28 MHz together with its harmonics. Instead, in fig. 5d, two modes are excited, one at about 5 MHz and another one at 552 kHz, together with the mechanical mode at 3.28 MHz. In theory, the modes around 3 MHz are breathing modes, the modes around 5 MHz are wine glass modes, whereas the modes in the kHz range involve the whole structure.

We can amplify these OMOs by pumping at higher frequency than the resonance (blue detuning). The cavity resonance enhances the red sideband [37,42] and suppresses both nonlinear optical effects and the blue sideband . Since, we are always scanning the pump from high to low frequency to achieve the thermal lock [16 di (2)][44], the mechanical oscillations result to be always amplified. Increasing the power at 200 mW and coupling close to the equator of a MBR (460 μm in diameter), the fundamental oscillation corresponds to a wine glass mode at 5.63 MHz with its higher harmonics (Fig.5a). In this case, high pump powers can excite higher order harmonics (up to 7th) and, in line with our previous simulations, the frequency of the oscillation increases with the decrease of the diameter.
In [46], we have evaluated the Q factor of the mechanical mode (close to $4 \cdot 10^3$, inset of Fig.5b) and estimated their stability. We monitored the ESA signal for more than 3 minutes, finding amplitude variations of the fundamental peak below 1.5 dB and position variations within 1.3 kHz [20]. After that, we studied the amplitude evolution of the fundamental peak as a function of the input power, which shows an oscillation threshold at about 40 mW, followed by a gain saturation at about 140mW (Fig.5c).

We have investigated the system exciting simultaneously two counter propagating WGMs at different wavelengths using two laser sources. One was excited by the amplified 1550 nm source, used to trigger the opto-mechanical oscillations, the other, by using a low power 1480 nm source (Anritsu TUNICS-Reference, probe laser) was used to interrogate the system. The mechanical modulation induced by the pump WGM was transferred to the probe WGM as consequence of the probe reading the MBR refractive index perturbations induced by the mechanical vibrations. This represents an interesting method to indirectly couple two WGMs, exploiting the significant overlap of the mechanical mode with two WGMs distributions. Simultaneously to the optomechanical vibrations, we can also observe optical nonlinear effects such as FWM, SRS and SBS. The nonlinear optical effects and OMOs are competitive processes [20,42] whose coexistence results to be dependent on the thermal locking conditions. These phenomena have been observed also in the first steps of the so-called “route to chaos” which indicates the evolution of the WGMR from the standard OMO regime to the chaotic one. In [46], we have presented the experimental results describing this transition evaluated for resonators of different sizes and increasing the input power. In particular, for a 520 μm diameter MBR, the route began with a periodic regime with only a few sharp peaks (Fig.6b), then a quasi-periodic doubling regime increasing the number of discrete lines

(Figure 6c), and finally, for input powers above 600 mW, a discrete oscillation on top of a continuum of frequencies (Fig.6d).

All these results agree very well with those previously reported for other WGMR geometries [35,43,47]. For larger MBRs (diameters above 600 μm), however, the transition is more abrupt, skipping the formation of the discrete peaks and falling directly into the frequency continuum. Finally, we have also shown that, in the pump-and-probe configuration, the WGM probe performs the same route of the pump. In this way the probe can be exploited to read-out the perturbations of the MBR refractive index and radius induced by the chaotic vibrations.

In conclusion, our review is aimed to report our results related to the coexistence of multi-resonant nonlinear optical phenomena (as Brillouin, Raman and Kerr effects) with the mechanical modes in MBRs, showing also how chaotic regimes can be reached by MBRs of different sizes. First, we have demonstrated that MBR are a very attractive class of WGMR for nonlinear optical emissions because of the dense spectra and the capacity of tailoring the dispersion thanks to its own geometry. Then, modeling the acoustic behavior of MBR by means of COMSOL Multiphysics, we have confirmed that its mechanical spectral density is very high, as for the optical ones. Depending on the coupling conditions and the locking of the resonance, we have experimentally observed OMO of either one mode, or several modes, in agreement with the observation in microtoroids [36]. Finally, we have presented the results of our experimental study on their chaos transition. The size of the bubble determines the route the system will take to reach the chaos. In particular, a quasiperiodic doubling for MBR with diameters below 600 μm and an abrupt transition for bigger ones. The same routes can be followed by a weak WGM probe thanks to the MBR capability of transferring chaos between different optical modes through the mechanical motion. In prospective, besides the fundamental aspect of our studies, our results pave the way to a new class of inertial devices which could be exploited also as sensing platforms [48].

Acknowledgement:

This work was financially supported by CNR bilateral projects with CONACYT and RFBR.

References:

[1] A.A. Savchenkov, A.B. Matsko, V.S. Ilchenko, L. Maleki, Optical resonators with ten million finesse, Opt. Express, OE. 15 (2007) 6768–6773. https://doi.org/10.1364/OE.15.006768.
[2] K.J. Vahala, Optical microcavities, Nature. 424 (2003) 839–846. https://doi.org/10.1038/nature01939.
[3] Y. Yang, X. Jiang, S. Kasumie, G. Zhao, L. Xu, J.M. Ward, L. Yang, S.N. Chormaic, Four-wave mixing parametric oscillation and frequency comb generation at visible wavelengths in a silica microbubble resonator, Opt. Lett., OL. 41 (2016) 5266–5269. https://doi.org/10.1364/OL.41.005266.
[4] J. Ward, Y. Yang, R. Madugani, S.N. Chormaic, Sensing and optomechanics using whispering gallery microbubble resonators, in: 2013 IEEE Photonics Conference, 2013: pp. 452–453. https://doi.org/10.1109/IPCon.2013.6656632.
[5] A. Chiasera, Y. Dumeige, P. Féron, M. Ferrari, Y. Jestin, G. Nunzi Conti, S. Pelli, S. Soria, G. c. Righini, Spherical whispering-gallery-mode microresonators, Laser & Photonics Reviews. 4 (2010) 457–482. https://doi.org/10.1002/lpor.200910016.
[6] M. Sumetsky, Whispering-gallery-bottle microcavities: the three-dimensional etalon, Opt. Lett., OL. 29 (2004) 8–10. https://doi.org/10.1364/OL.29.000008.
[7] S. Berneschi, D. Farnesi, F. Cosi, G.N. Conti, S. Pelli, G.C. Righini, S. Soria, High Q silica microbubble resonators fabricated by arc discharge, Opt. Lett., OL. 36 (2011) 3521–3523. https://doi.org/10.1364/OL.36.003521.
[8] M. Sumetsky, Y. Dulashko, R.S. Windeler, Optical microbubble resonator, Opt. Lett., OL. 35 (2010) 898–900. https://doi.org/10.1364/OL.35.000898.
[9] M. Li, X. Wu, L. Liu, X. Fan, L. Xu, Self-Referencing Optofluidic Ring Resonator Sensor for Highly Sensitive Biomolecular Detection, Anal. Chem. 85 (2013) 9328–9332. https://doi.org/10.1021/ac402174x.
[10] K.H. Kim, X. Fan, Surface sensitive microfluidic optomechanical ring resonator sensors, Appl. Phys. Lett. 105 (2014) 191101. https://doi.org/10.1063/1.4901067.
[11] J.M. Ward, Y. Yang, S.N. Chormaic, Highly Sensitive Temperature Measurements With Liquid-Core Microbubble Resonators, IEEE Photonics Technology Letters. 25 (2013) 2350–2353. https://doi.org/10.1109/LPT.2013.2283732.

[12] Y. Yang, J. Ward, S.N. Chormaic, Quasi-droplet microbubbles for high resolution sensing applications, Opt. Express, OE. 22 (2014) 6881–6898. https://doi.org/10.1364/OE.22.006881.
[13] K. Han, K. Zhu, G. Bahl, Opto-mechano-fluidic viscometer, Appl. Phys. Lett. 105 (2014) 014103. https://doi.org/10.1063/1.4887369.
[14] N. Riesen, W.Q. Zhang, T.M. Monro, Dispersion in silica microbubble resonators, Opt. Lett., OL. 41 (2016) 1257–1260. https://doi.org/10.1364/OL.41.001257.
[15] R. Henze, T. Seifert, J. Ward, O. Benson, Tuning whispering gallery modes using internal aerostatic pressure, Opt. Lett., OL. 36 (2011) 4536–4538. https://doi.org/10.1364/OL.36.004536.
[16] Q. Lu, S. Liu, X. Wu, L. Liu, L. Xu, Stimulated Brillouin laser and frequency comb generation in high-Q microbubble resonators, Opt. Lett., OL. 41 (2016) 1736–1739. https://doi.org/10.1364/OL.41.001736.
[17] D. Farnesi, G. Righini, G. Nunzi Conti, S. Soria, Efficient frequency generation in phoXonic cavities based on hollow whispering gallery mode resonators, Sci Rep. 7 (2017) 44198. https://doi.org/10.1038/srep44198.
[18] J.M. Ward, Y. Yang, S. Nic Chormaic, Glass-on-Glass Fabrication of Bottle-Shaped Tunable Microlasers and their Applications, Sci Rep. 6 (2016) 25152. https://doi.org/10.1038/srep25152.
[19] G. Bahl, K.H. Kim, W. Lee, J. Liu, X. Fan, T. Carmon, Brillouin cavity optomechanics with microfluidic devices, Nat Commun. 4 (2013) 1994. https://doi.org/10.1038/ncomms2994.
[20] X. Roselló-Mechó, D. Farnesi, G. Frigenti, A. Barucci, A. Fernández-Bienes, T. García-Fernández, F. Ratto, M. Delgado-Pinar, M.V. Andrés, G. Nunzi Conti, S. Soria, Parametrical Optomechanical Oscillations in PhoXonic Whispering Gallery Mode Resonators, Sci Rep. 9 (2019) 7163. https://doi.org/10.1038/s41598-019-43271-x.
[21] I.S. Grudinin, A.B. Matsko, L. Maleki, Brillouin Lasing with a CaF2 Whispering Gallery Mode Resonator, Phys. Rev. Lett. 102 (2009) 043902. https://doi.org/10.1103/PhysRevLett.102.043902.
[22] G. Bahl, M. Tomes, F. Marquardt, T. Carmon, Observation of spontaneous Brillouin cooling, Nature Phys. 8 (2012) 203–207. https://doi.org/10.1038/nphys2206.
[23] M. Maldovan, E.L. Thomas, Simultaneous localization of photons and phonons in two-dimensional periodic structures, Appl. Phys. Lett. 88 (2006) 251907. https://doi.org/10.1063/1.2216885.
[24] Q. Rolland, M. Oudich, S. El-Jallal, S. Dupont, Y. Pennec, J. Gazalet, J.C. Kastelik, G. Lévêque, B. Djafari-Rouhani, Acousto-optic couplings in two-dimensional phoxonic crystal cavities, Appl. Phys. Lett. 101 (2012) 061109. https://doi.org/10.1063/1.4744539.
[25] R. Boyd, Nonlinear Optics, 2nd Edition, Academic Press, San Diego, 2003. https://doi.org/10.1016/B978-0-12-121682-5.X5000-7.
[26] H. Lee, T. Chen, J. Li, K.Y. Yang, S. Jeon, O. Painter, K.J. Vahala, Chemically etched ultrahigh-Q wedge-resonator on a silicon chip, Nature Photon. 6 (2012) 369–373. https://doi.org/10.1038/nphoton.2012.109.
[27] B.J. Eggleton, C.G. Poulton, R. Pant, Inducing and harnessing stimulated Brillouin scattering in photonic integrated circuits, Adv. Opt. Photon., AOP. 5 (2013) 536–587. https://doi.org/10.1364/AOP.5.000536.
[28] M. Asano, Y. Takeuchi, S.K. Ozdemir, R. Ikuta, L. Yang, N. Imoto, T. Yamamoto, Stimulated Brillouin scattering and Brillouin-coupled four-wave-mixing in a silica microbottle resonator, Opt. Express, OE. 24 (2016) 12082–12092. https://doi.org/10.1364/OE.24.012082.
[29] G. Lin, S. Diallo, K. Saleh, R. Martinenghi, J.-C. Beugnot, T. Sylvestre, Y.K. Chembo, Cascaded Brillouin lasing in monolithic barium fluoride whispering gallery mode resonators, Appl. Phys. Lett. 105 (2014) 231103. https://doi.org/10.1063/1.4903516.
[30] C. Guo, K. Che, Z. Cai, S. Liu, G. Gu, C. Chu, P. Zhang, H. Fu, Z. Luo, H. Xu, Ultralow-threshold cascaded Brillouin microlaser for tunable microwave generation, Opt. Lett., OL. 40 (2015) 4971–4974. https://doi.org/10.1364/OL.40.004971.
[31] G. Lin, S. Diallo, J.M. Dudley, Y.K. Chembo, Universal nonlinear scattering in ultra-high Q whispering gallery-mode resonators, Opt. Express, OE. 24 (2016) 14880–14894. https://doi.org/10.1364/OE.24.014880.
[32] W. Liang, A.A. Savchenkov, Z. Xie, J.F. McMillan, J. Burkhart, V.S. Ilchenko, C.W. Wong, A.B. Matsko, L. Maleki, Miniature multioctave light source based on a monolithic microcavity, Optica, OPTICA. 2 (2015) 40–47. https://doi.org/10.1364/OPTICA.2.000040.
[33] D. Farnesi, A. Barucci, G.C. Righini, G.N. Conti, S. Soria, Generation of hyper-parametric oscillations in silica microbubbles, Opt. Lett., OL. 40 (2015) 4508–4511. https://doi.org/10.1364/OL.40.004508.

[34] G. Bahl, J. Zehnpfennig, M. Tomes, T. Carmon, Stimulated optomechanical excitation of surface acoustic waves in a microdevice, Nat Commun. 2 (2011) 403. https://doi.org/10.1038/ncomms1412.
[35] T. Carmon, M.C. Cross, K.J. Vahala, Chaotic Quivering of Micron-Scaled On-Chip Resonators Excited by Centrifugal Optical Pressure, Phys. Rev. Lett. 98 (2007) 167203. https://doi.org/10.1103/PhysRevLett.98.167203.
[36] T.J. Kippenberg, H. Rokhsari, T. Carmon, A. Scherer, K.J. Vahala, Analysis of Radiation-Pressure Induced Mechanical Oscillation of an Optical Microcavity, Phys. Rev. Lett. 95 (2005) 033901. https://doi.org/10.1103/PhysRevLett.95.033901.
[37] M. Asano, Y. Takeuchi, W. Chen, Ş.K. Özdemir, R. Ikuta, N. Imoto, L. Yang, T. Yamamoto, Observation of optomechanical coupling in a microbottle resonator, Laser & Photonics Reviews. 10 (2016) 603–611. https://doi.org/10.1002/lpor.201500243.
[38] V.B. Braginsky, S.E. Strigin, S.P. Vyatchanin, Parametric oscillatory instability in Fabry–Perot interferometer, Physics Letters A. 287 (2001) 331–338. https://doi.org/10.1016/S0375-9601(01)00510-2.
[39] H. Rokhsari, T.J. Kippenberg, T. Carmon, K.J. Vahala, Radiation-pressure-driven micro-mechanical oscillator, Opt. Express, OE. 13 (2005) 5293–5301. https://doi.org/10.1364/OPEX.13.005293.
[40] T. Carmon, H. Rokhsari, L. Yang, T.J. Kippenberg, K.J. Vahala, Temporal Behavior of Radiation-Pressure-Induced Vibrations of an Optical Microcavity Phonon Mode, Phys. Rev. Lett. 94 (2005) 223902. https://doi.org/10.1103/PhysRevLett.94.223902.
[41] T.J. Kippenberg, K.J. Vahala, Cavity Opto-Mechanics, Opt. Express, OE. 15 (2007) 17172–17205. https://doi.org/10.1364/OE.15.017172.
[42] R. Suzuki, T. Kato, T. Kobatake, T. Tanabe, Suppression of optomechanical parametric oscillation in a toroid microcavity assisted by a Kerr comb, Opt. Express, OE. 25 (2017) 28806–28816. https://doi.org/10.1364/OE.25.028806.
[43] F. Monifi, J. Zhang, Ş.K. Özdemir, B. Peng, Y. Liu, F. Bo, F. Nori, L. Yang, Optomechanically induced stochastic resonance and chaos transfer between optical fields, Nature Photon. 10 (2016) 399–405. https://doi.org/10.1038/nphoton.2016.73.
[44] T. Carmon, L. Yang, K.J. Vahala, Dynamical thermal behavior and thermal self-stability of microcavities, Opt. Express, OE. 12 (2004) 4742–4750. https://doi.org/10.1364/OPEX.12.004742.
[45] A. Cosci, F. Quercioli, D. Farnesi, S. Berneschi, A. Giannetti, F. Cosi, A. Barucci, G.N. Conti, G. Righini, S. Pelli, Confocal reflectance microscopy for determination of microbubble resonator thickness, Opt. Express, OE. 23 (2015) 16693–16701. https://doi.org/10.1364/OE.23.016693.
[46] X. Rosello-Mecho, G. Frigenti, D. Farnesi, M. Delgado-Pinar, M.V. Andrés, F. Ratto, N. Conti, S. Soria, Microbubble PhoXonic resonators: Chaos transition and transfer, Chaos, Solitons & Fractals. 154 (2022) 111614. https://doi.org/10.1016/j.chaos.2021.111614.
[47] L. Bakemeier, A. Alvermann, H. Fehske, Route to Chaos in Optomechanics, Phys. Rev. Lett. 114 (2015) 013601. https://doi.org/10.1103/PhysRevLett.114.013601.
[48] G. Frigenti, L. Cavigli, A. Fernández-Bienes, F. Ratto, S. Centi, T. García-Fernández, G. Nunzi Conti, S. Soria, Resonant Microbubble as a Microfluidic Stage for All-Optical Photoacoustic Sensing, Phys. Rev. Applied. 12 (2019) 014062. https://doi.org/10.1103/PhysRevApplied.12.014062.

Figures:

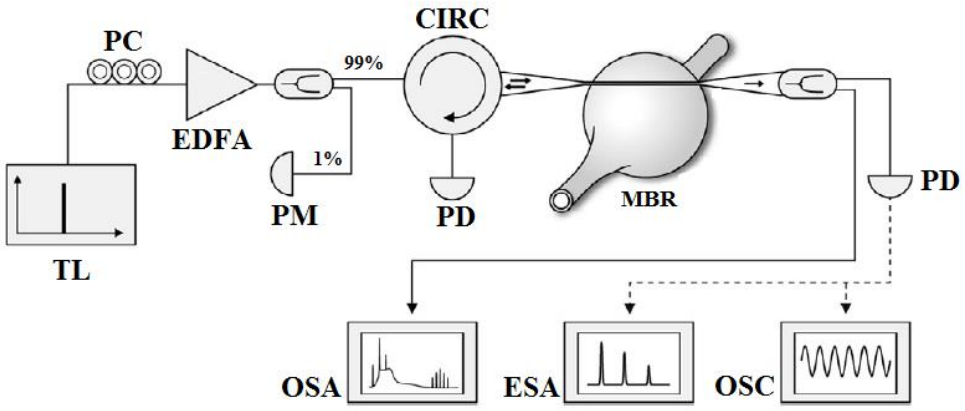

Fig. 1. Experimental setup scheme for exciting and measuring optomechanical vibrations induced by radiation pressure. Abbreviations: TL: tunable laser diode, PM: power meter PC: polarization controller, EDFA: erbium doped fiber amplifier, OSA: optical spectrum analyzer, ESA: electrical spectrum analyzer, OSC: oscilloscope, PD: photodiode.

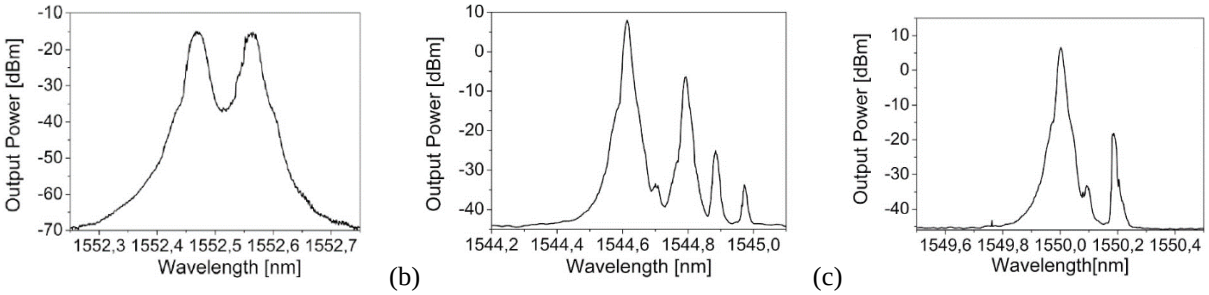

(a) (b) (c)

Figure 2. (a) First order SBS Stokes lines in backward direction for a 475 μm diameter MBR with a wall thickness of about 3–4 μm; (b) Cascaded forward SBS in a 675 μm diameter MBR and wall thickness of about 2 μm; (c) Cascaded SBS up to the 2nd order [17].

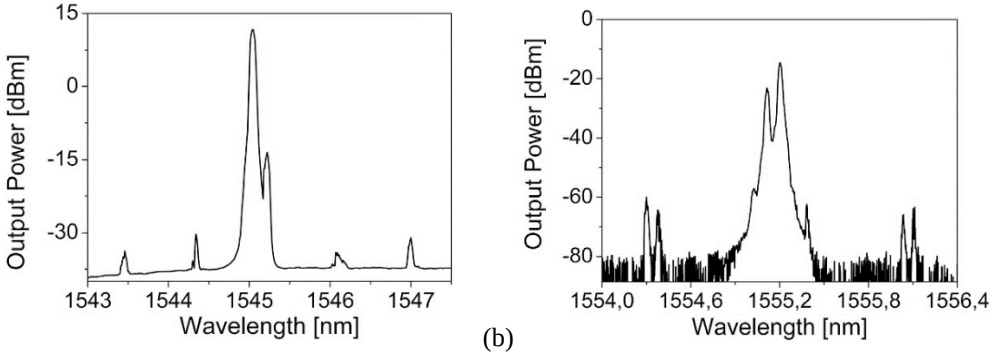

(a) (b)

Figure 3. SBS and degenerated FWM emissions in forward (a) and backward (b) direction [17].

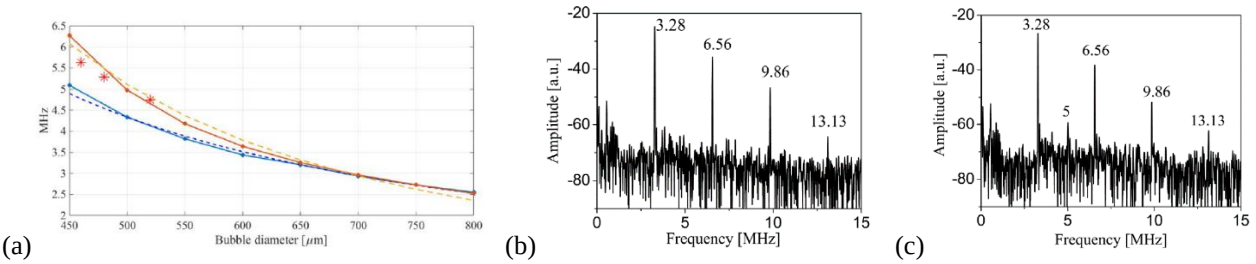

Figure 4. (a) COMSOL Multiphysics numerical simulations of the MBR diameter effect on the excitation of the mechanical oscillations for higher frequency modes. Experimental oscillations at 72 mW and 1553.476 nm for one single family (c) and two different families (d) of excited modes [20].

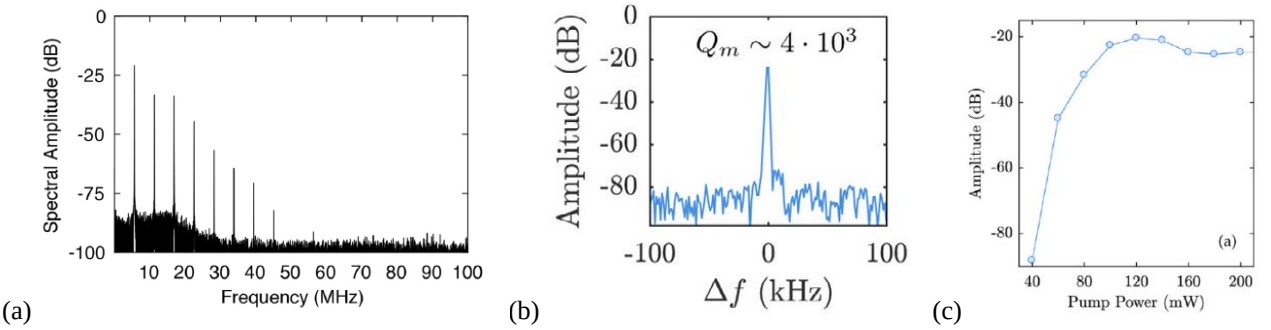

Figure 5. (a) Mechanical oscillations measured at the ESA of first excited mechanical mode and its harmonics for a bubble of 460 μm of diameter at 200 mW [20]; (b) Mechanical Q-factor; (c) Fundamental peak amplitude evolution as a function of the pump power.

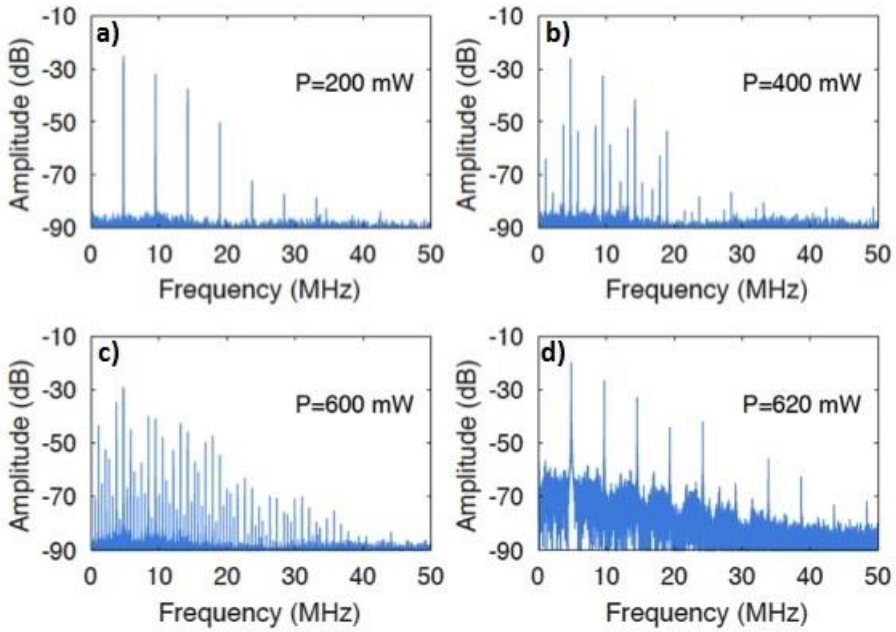

Fig. 6. Transition to chaos increasing the launched power is increased: (a) 200mW, (b) 400mW, (c)600mW and (d) 620mW. The fundamental mode is centered at 4.74 MHz.